Geophysical Research Letters

RESEARCH LETTER
10.1029/2020GL091266

Quantifying Nitrous Oxide Emissions in the U.S. Midwest: A Top-Down Study Using High Resolution Airborne In-Situ Observations

Maximilian Eckl[1], Anke Roiger[1], Julian Kostinek[1], Alina Fiehn[1], Heidi Huntrieser[1], Christoph Knote[2], Zachary R. Barkley[3], Stephen M. Ogle[4], Bianca C. Baier[5,6], Colm Sweeney[6], and Kenneth J. Davis[3,7]

[1]Deutsches Zentrum für Luft- und Raumfahrt (DLR), Institut für Physik der Atmosphäre, Oberpfaffenhofen, Germany, [2]Meteorological Institute, Ludwig-Maximilians-University (LMU), Munich, Germany, [3]Department of Meteorology and Atmospheric Science, Pennsylvania State University, University Park, PA, USA, [4]Natural Resource Ecology Laboratory, Colorado State University, Fort Collins, CO, USA, [5]Cooperative Institute for Research in Environmental Sciences, University of Colorado-Boulder, Boulder, CO, USA, [6]NOAA Global Monitoring Laboratory, Boulder, CO, USA, [7]Earth and Environmental Systems Institute, Pennsylvania State University, University Park, PA, USA

Key Points:

- Within the ACT-America project, we gathered a unique airborne in-situ N_2O data set over the U.S. Midwest with enhancements up to 9 ppb
- N_2O emissions in the U.S. Midwest were on average 0.42 ± 0.28 nmol m^{-2} s^{-1} in October 2017 and 1.06 ± 0.57 nmol m^{-2} s^{-1} in June to July 2019
- Bottom-up estimates from EDGAR and DayCent underestimate U.S. Midwest N_2O emissions by factors up to 20

Supporting Information:

Supporting Information may be found in the online version of this article.

Correspondence to:

M. Eckl,
Maximilian.Eckl@dlr.de

Citation:

Eckl, M., Roiger, A., Kostinek, J., Fiehn, A., Huntrieser, H., Knote, C., et al. (2021). Quantifying nitrous oxide emissions in the U.S. Midwest: A top-down study using high resolution airborne in-situ observations. *Geophysical Research Letters*, *48*, e2020GL091266. https://doi.org/10.1029/2020GL091266

Received 14 OCT 2020
Accepted 5 JAN 2021

Abstract The densely farmed U.S. Midwest is a prominent source of nitrous oxide (N_2O) but top-down and bottom-up N_2O emission estimates differ significantly. We quantify Midwest N_2O emissions by combining observations from the Atmospheric Carbon and Transport-America campaign with model simulations to scale the Emissions Database for Global Atmospheric Research (EDGAR). In October 2017, we scaled agricultural EDGAR v4.3.2 and v5.0 emissions by factors of 6.3 and 3.5, respectively, resulting in 0.42 nmol m^{-2} s^{-1} Midwest N_2O emissions. In June/July 2019, a period when extreme flooding was occurring in the Midwest, agricultural scaling factors were 11.4 (v4.3.2) and 9.9 (v5.0), resulting in 1.06 nmol m^{-2} s^{-1} Midwest emissions. Uncertainties are on the order of 50 %. Agricultural emissions estimated with the process-based model DayCent (Daily version of the CENTURY ecosystem model) were larger than in EDGAR but still substantially smaller than our estimates. The complexity of N_2O emissions demands further studies to fully characterize Midwest emissions.

Plain Language Summary Nitrous oxide (N_2O) is the third most important anthropogenic greenhouse gas contributing to the warming of the planet and the dominant man-made ozone-depleting substance in the stratosphere. Its atmospheric concentrations have been rising since industrialization mainly due to an increase in anthropogenic sources, with agriculture being the dominant source. The densely farmed U.S. Midwest plays an important role in the global N_2O budget. However, previous studies that have collected observations of N_2O indicate that estimates of surface emissions in the Midwest are substantially underestimating the truth. In this study, we combine unique aircraft-based N_2O measurements and model simulations to quantify Midwest emissions in October 2017 and June/July 2019. Agricultural inventory estimates had to be increased by factors up to 20 to match observations, revealing a large underestimation in current inventories. An extreme flooding event in 2019 when the summer observations occurred may be responsible for some of this discrepancy. Estimations of soil N_2O emissions calculated with a state-of-the-art biogeochemical model show less underestimation but are still too low compared to the fluxes derived from the aircraft observational data.

1. Introduction

Nitrous oxide (N_2O) is the third most important anthropogenic greenhouse gas (GHG) in terms of long-term radiative forcing (Myhre et al., 2013) and is the dominant ozone-depleting substance in the stratosphere (Ravishankara et al., 2009). Global N_2O concentrations are 333 ppb as of April 2020, approximately a 20 % increase since preindustrial times (MacFarling Meure et al., 2006; NOAA-ESRL, 2020). Anthropogenic sources like agriculture and fossil fuel combustion contribute to this trend (Ciais et al., 2013). In recent years, those N_2O emissions have increased at a higher rate than expected (Thompson et al., 2019; Tian et al., 2020). Agricultural soil management associated with reactive forms of nitrogen (N) (i.e., mineral fertilizer, livestock manure additions, and legumes) accounts for half of global N_2O emissions (Paustian

et al., 2016). Analyses of the isotopic composition of N_2O indicate that the observed rise in global atmospheric N_2O concentrations is mainly caused by the increased application of N-fertilizers (Park et al., 2012).

Bottom-up estimates, such as the Emissions Database for Global Atmospheric Research (EDGAR, 2020), use emission factors and activity data to calculate emissions. Agricultural practices (e.g., fertilizer application, crop type) as well as meteorological and soil conditions (e.g., precipitation, soil moisture) directly influence emissions, resulting in large temporal variability in N_2O surface fluxes (Stehfest & Bouwman, 2006). Process-based models like DayCent (Daily version of the CENTURY ecosystem model) provide a more sophisticated approach for estimation of N_2O emission by simulating soil processes based on various environmental drivers. Nevertheless, fluxes at regional scale are still highly uncertain due to insufficient direct observations (Reay et al., 2012).

The U.S. Midwest is one of the most intensively cultivated agricultural regions worldwide (FAO, 2020; USDA-NASS, 2020), thus contributing significantly to global anthropogenic N_2O emissions (Miller et al., 2012). Previous top-down studies indicate that emissions in the Midwest are underestimated by EDGAR, but are highly uncertain on the magnitude of this underestimation (Chen et al., 2016; Fu et al., 2017; Griffis et al., 2013; Kort et al., 2008; Miller et al., 2012). Kort et al. (2008) showed that EDGAR version 32FT2000 underestimates emissions in May to June 2003 by a factor of 2.62 over the central U.S. and southern Canada. Miller et al. (2012) derived scaling factors of 6.1 and 10.1 for EDGAR version 4 for June 2004 and June 2008, respectively. Fu et al. (2017) concluded even higher scaling factors for agricultural EDGAR version 4.2 emissions in the Corn Belt region of the Midwest, with scaling factors of 19.0–28.1 in June 2010. These described top-down studies used tall tower measurements, characterized by long time series over several months but limited in their spatial coverage. Only Kort et al. (2008) used aircraft-based flask measurements, which provide some spatial (central U.S. and southern Canada) but limited temporal (May to June 2003) coverage. The large range in the quantitative results show that Midwest N_2O surface fluxes are underestimated by EDGAR inventories, but their true values are highly uncertain.

In this study, we quantify N_2O emissions for several flights conducted in parts of the U.S. Midwest in October 2017 and June/July 2019 with a top-down approach. Unlike previous studies which have relied on observations with limited spatial coverage, this study uses continuous airborne in-situ measurements of N_2O. By combining these observations with forward model simulations, we optimize agricultural fluxes from EDGAR version 4.3.2 and version 5.0 to quantify Midwest N_2O emissions. The employed method was already successfully applied in several methane top-down studies (Barkley et al., 2017, 2019a, 2019b). The derived emission rates are finally compared to flux estimates of direct soil emissions produced with EDGAR and the biogeochemical model DayCent (Del Grosso et al., 2001, 2011; Parton et al., 1998).

2. Data and Methods

2.1. Observational Data

We use measurements from the Atmospheric Carbon and Transport-America (ACT-America) campaign. During the fall 2017 (October 10–November 13) and summer 2019 (June 17–July 27) field deployments, we collected ~60 h of in-situ data onboard NASA's C-130 with an Aerodyne Quantum Cascade Laser Spectrometer (QCLS) measuring N_2O mole fractions (among others) at 2 Hz with an uncertainty of 0.8 ppb (Kostinek et al., 2019). Every 3–10 min in-flight calibrations were performed using standards that were cross-calibrated after the campaign against NOAA/GML standards traceable to the NOAA-2006A scale (Hall et al., 2007). Additionally, during each flight 6–12 whole-air flask samples were taken by NOAA/GML and analyzed for trace gases including N_2O with an uncertainty of 0.4 ppb (Baier et al., 2020; Sweeney et al., 2015, 2018). Those were merged into the QCLS time series to fill any data gaps.

For this study, we selected four flights from 2017 (October) and six flights from 2019 (June/July). For each flight, the C-130 flew transects well within the planetary boundary layer (PBL) (~1,000 ft above ground level (AGL)) for at least 45 min during which air above the Midwest was sampled. Figure 1a shows the selected transects, color-coded with observed N_2O dry air mole fractions. Mole fractions up to 341 ppb were measured (Figure 1b). We are not aware of comparable continuous N_2O measurements spanning most of the Midwest across two seasons, highlighting the unique opportunity to quantify Midwest emissions with these data.

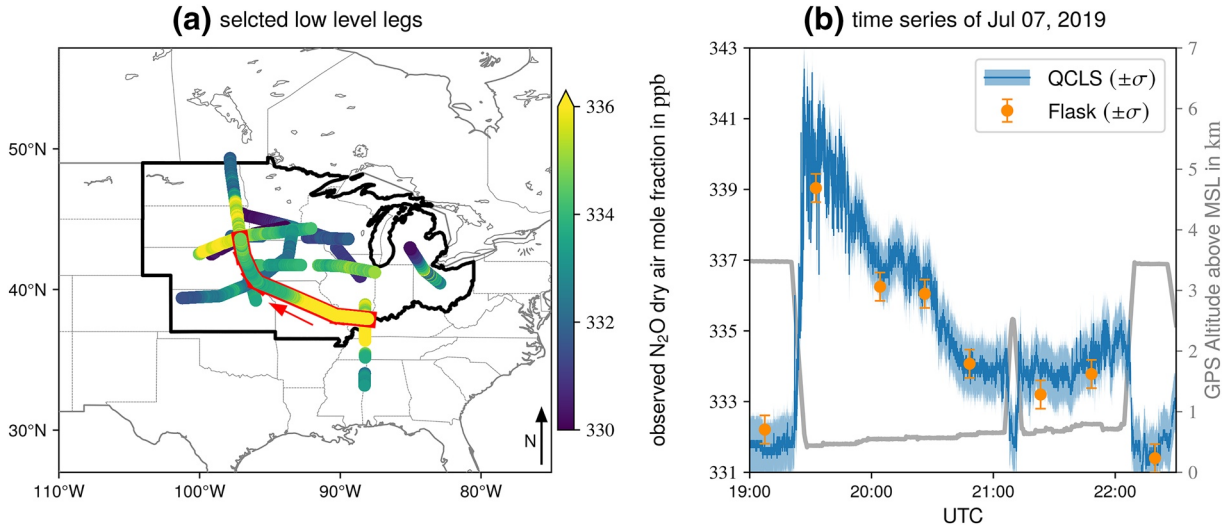

Figure 1. (a) Selected PBL transects (at ~1,000 ft AGL) of the ACT-America campaigns in 2017 and 2019, color-coded with observed N_2O dry air mole fractions. The Midwest region used for emission estimation in the model is encircled by a thick black line. (b) Time series of N_2O dry air mole fraction of the flight on July 7, 2019 with error bars indicating ±0.8 ppb and coincident NOAA/GML flask measurements of N_2O (±0.4 ppb). The corresponding transect in (a) is encircled in red and was flown in direction of the red arrow. PBL, planetary boundary layer; AGL, above ground level.

2.2. Model Setup

The Weather Research and Forecasting model with chemistry enabled (Grell et al., 2005) is used to propagate N_2O enhancements emitted from emission inventories (Section 2.3) through the atmosphere. Initial N_2O concentrations and the inflow at the boundaries of the model domain are set to zero. Thus, we simulate only enhancements caused by emissions within the model domain. We treat N_2O as a passive tracer due to its long atmospheric lifetime of ~116 years (Prather et al., 2015). The model domain consists of an outer and inner domain with a horizontal resolution of 15 km × 15 km and 3 km × 3 km, respectively. The outer domain, centered over the Midwest, covers nearly the whole continental U.S., northern Mexico, and southern Canada (Figure 2a), whereas the extent and position of the inner domain is chosen separately for each flight so that the PBL transects are spaciously encapsulated. We perform each simulation with three different meteorological initial and boundary conditions: The fifth generation atmospheric reanalysis data (ERA5, 2017; Hersbach et al., 2020), the North American Regional Reanalysis (NARR, 2005), and the Global Data Assimilation System Final analysis (GDAS-FNL, 2015). As in Barkley et al. (2019a), we use these different simulations to estimate model transport errors (Díaz-Isaac et al., 2018). The SupportingInformation(SI) provides additional information about the model setup.

2.3. Emission Inventories

The prior N_2O emission estimates for the optimization were obtained from EDGAR version 4.3.2 (EDGAR4.3.2, 2017; Janssens-Maenhout et al., 2019) and version 5.0 (Crippa et al., 2020;EDGAR5.0, 2019). For this study the different sectors in the inventories were merged into three main sectors: agricultural E_{AGR}, anthropogenic nonagricultural E_{nonAGR}, and natural emissions E_N (see SI). We assume that these three sectors cover all N_2O emissions in the model domain. EDGAR4.3.2 and EDGAR5.0 provide monthly resolved N_2O fluxes from anthropogenic sources (E_{AGR} and E_{nonAGR}) on a 0.1° × 0.1° grid for 2012 and 2015, respectively, but do not include fluxes from natural sources. Hence, we supplemented both versions with yearly E_N on a 1° × 1° grid from EDGAR version 2.0 (EDGAR2; Olivier et al., 1996, 1999).

With the process-based, biogeochemical model DayCent we estimated daily direct N_2O soil emissions from cropland and grassland on a 0.5° × 0.5° grid in the Midwest from 2011 to 2015, which were aggregated to a monthly time step. The model simulates fluxes of carbon and nitrogen between the atmosphere, vegetation, and soil thus deriving N_2O emissions. Incorporating several environmental drivers, including weather patterns, agricultural practices, soil characteristics, and crop features, this approach provides a more

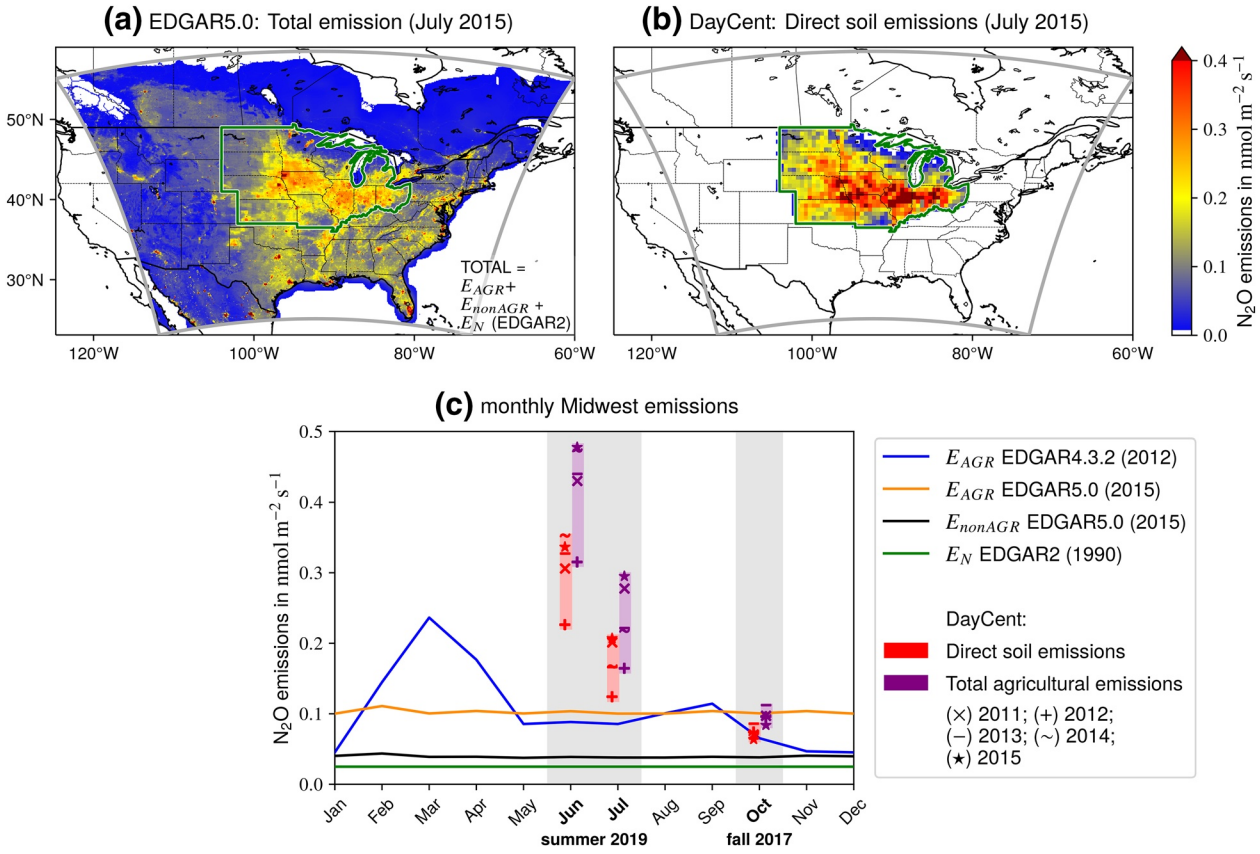

Figure 2. (a) EDGAR5.0 N_2O emissions (plus EDGAR2 E_N) within the model domain (gray box). The Midwest is encircled in green. (b) Direct soil emissions in July 2015 estimated with DayCent. (c) Monthly Midwest emissions. E_{nonAGR} in EDGAR4.3.2 is almost identical to EDGAR5.0. Total agricultural DayCent emissions are estimated utilizing the EPA GHG inventory (Section 2.3).

sophisticated estimate of soil emissions than the emission factor-based EDGAR. The GHG inventory of the United States Environmental Protection Agency (EPA, 2020) uses DayCent estimates of direct soil emissions for emission reporting of agricultural soil N_2O to the UN Framework Convention on Climate Change. DayCent does not calculate emissions from manure management, agricultural waste burning, indirect soil emissions, and those associated with minor crops such as vegetables. The EPA inventory quantifies these sources with an emission factor approach. We estimate their contribution by employing the yearly, national estimates from EPA, calculating their fraction of the EPA direct soil emissions, and adding them to our monthly estimates. As a result, our DayCent inventory accounts for the total agricultural emissions, but not the spatial distribution of agricultural sources which are not estimated by DayCent. A qualitative comparison of EDGAR emission maps supports the underlying assumption that the spatial distribution of soil and other agricultural emissions are similar.

2.4. Optimization Technique

To solve for N_2O emissions, we use an approach similar to the optimization described in Barkley et al. (2017). First, we calculate the observed N_2O enhancements by subtracting a background from the measured absolute mole fraction. For each campaign we derive one background by taking the second percentile of all PBL transects of the entire campaign (see SI). The background is defined campaign-wise rather than transect-wise because during some transects we were not able to measure background mole fractions as we started a transect within a plume and did not exit the plume inside of the PBL (Figure 1b).

We then compare modeled N_2O enhancements from our prior emissions ($E_{AGR} + E_{nonAGR} + E_N$) to the observed enhancements. Differences between both are then minimized for each flight by scaling agricultural

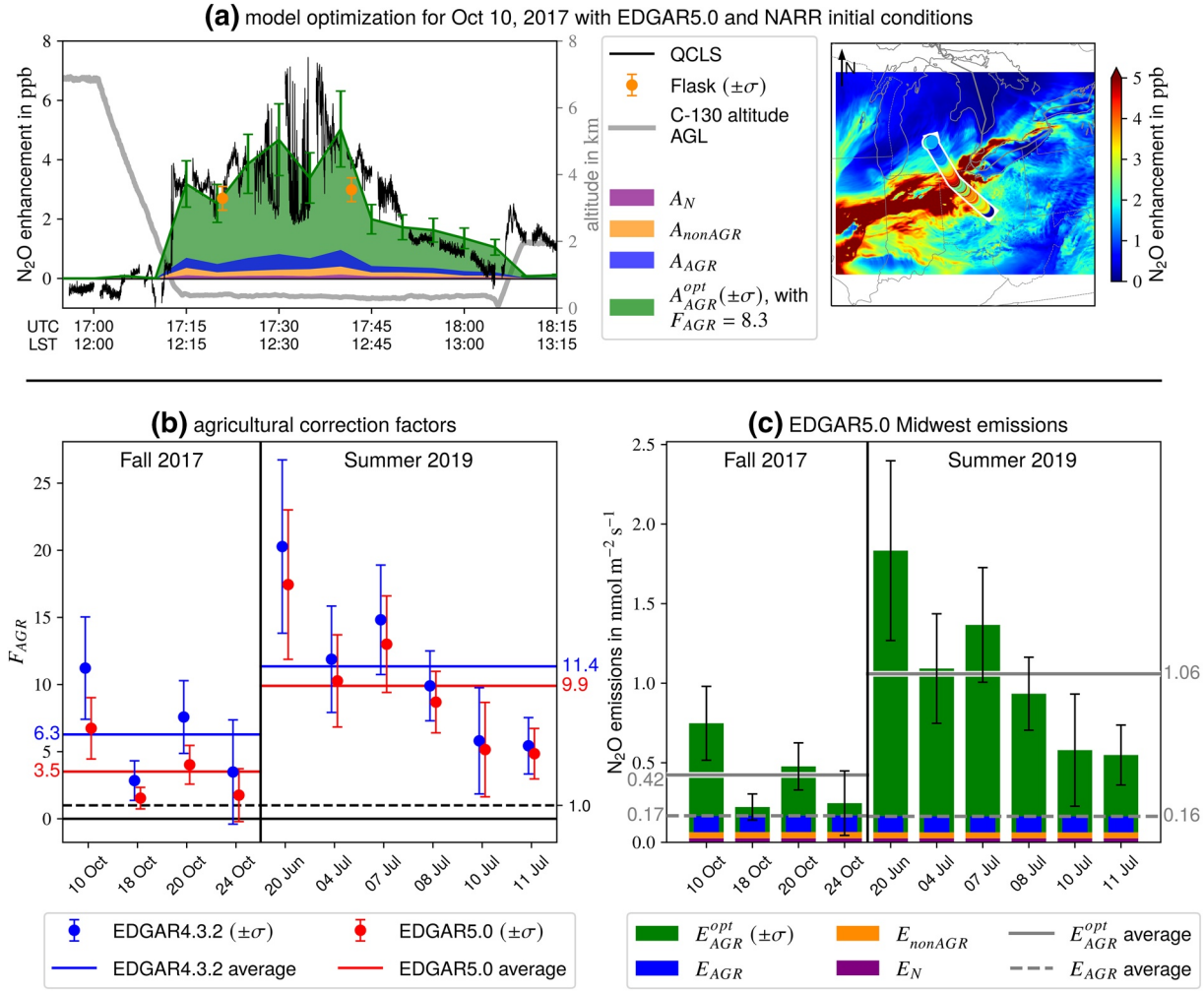

Figure 3. (a) Sample model optimization for October 10, 2017 with EDGAR5.0 (plus EDGAR2 E_N) and NARR initial conditions. The left panel shows the prior and optimized modeled N_2O enhancements along the flight track together with observed enhancements. The right panel shows a map of optimized modeled N_2O enhancements (from $E^{opt}_{AGR} + E_{nonAGR} + E_N$) at 300 m AGL at 17:30 UTC and the flight track color-coded with the observed enhancements. (b) Mean and standard deviation of agricultural correction factors F_{AGR} for the investigated research flights resulting from Monte Carlo simulations. (c) EDGAR5.0 Midwest N_2O emissions with optimized and prior E_{AGR}. AGL, above ground level.

emissions E_{AGR} with a factor F_{AGR} thus quantifying emissions. This process relies on the assumption that the discrepancy between model and observation is primarily driven by errors in E_{AGR}. As agricultural emissions are the dominant N_2O source in our flights, we assume that errors in E_{nonAGR} and E_N are inconsequential to the overall solution. The complexity of N_2O soil emissions suggests that E_{AGR} exhibits a much higher uncertainty than other sources (Butterbach-Bahl et al., 2013), supporting the presented approach.

As an equation, this optimization technique is described by calculating F_{AGR} through the minimization of the following cost function:

$$J(F_{AGR}) = \mid A_{obs} - \underbrace{\left(F_{AGR} \cdot A_{AGR} + A_{nonAGR} + A_N\right)}_{=A_{mod}(F_{AGR})} \mid \tag{1}$$

A_{obs} and A_{mod} are the time integral along a transect of observed and modeled enhancements, respectively (e.g., area below graph in Figure 3a). A_{mod} consists of an agricultural portion A_{AGR} scaleable with F_{AGR}, a non-agricultural anthropogenic portion A_{nonAGR}, and a natural portion A_N. We compare integrals rather than enhancements because we are interested in the amount of N_2O emitted to the atmosphere. Neither the model transport nor the inventory is perfect and even small uncertainties in either of them could cause a

shift or deformation in the alignment of the modeled plume relative to the observed plume. By minimizing the difference in the total N_2O enhancements rather than the point-by-point absolute error, we preserve the capability to solve for total N_2O emissions even when the modeled and observed plumes do not align. Due to the linearity between A_{AGR} and the area averaged E_{AGR} (see SI), a F_{AGR} derived with Equation 1 denotes a F_{AGR}-folded E_{AGR}.

2.5. Uncertainty Assessment

We adopted the method of Barkley et al. (2019a) to assess uncertainties in our solutions. F_{AGR} is affected by uncertainties in the following variables:

1. observed background mole fraction
2. A_{nonAGR}
3. A_N
4. model transport
5. model wind speed and PBL height (PBLH)
6. spatial distribution in EDGAR emissions

We quantify the influence of uncertainties 1–4 with a Monte Carlo approach. For each flight, we repeat the optimization 10,000 times with a perturbed background mole fraction, A_{nonAGR}, and A_N. For the background we add a normal random number with $\mu = 0$ ppb and $\sigma = \pm 0.5$ ppb for 2017 and $\sigma = \pm 0.9$ ppb for 2019 to the observation derived value. A_{nonAGR} and A_N are independently multiplied by a factor drawn from a normal distribution with $\mu = 1.0$ and $\sigma = \pm 0.21$ and $\sigma = \pm 0.42$, respectively. To account for the model transport error, we randomly select one of the three model runs with different meteorological initial and boundary conditions, creating variability in the plume shape. The resulting spread in F_{AGR} is used as its uncertainty. Explanations of the used uncertainties are in the SI.

The modeled wind speed and PBLH uncertainty (source 5) cannot be covered by the Monte Carlo simulation. Errors in these variables cause lower or higher simulated enhancements thus producing biases. Following Barkley et al. (2017), we correct for those biases by applying a correction factor based on the differences between the modeled and observed wind speed and PBLH. On average, the modeled wind speed and PBLH is 8 % and 3 % higher than observations, respectively. The impact of this correction on our results is insignificant (see SI).

Our final source of uncertainty relates to errors in the spatial distribution of the fluxes in the prior inventory and is difficult to quantify. However, the mapping of emissions in EDGAR is based on several high-resolution proxy data sets (Janssens-Maenhout et al., 2019). For this reason, we assume its spatial errors to be small. Given the insignificant difference between modeled and observed wind speeds and PBLH, the good agreement between modeled and measured plume structures support this assumption (see SI). Furthermore, because we quantify large areas and not point sources, slight misplacement in the inventory would only marginally affect our results. At the same time, missing or strongly misplaced fluxes would produce errors that are not considered in this study.

3. Results and Discussion

3.1. Emission Inventory Comparison

Figure 2a shows prior July N_2O emissions in the outermost model domain from anthropogenic EDGAR5.0 and natural EDGAR2 sources. Compared to EDGAR4.3.2 no significant differences in the spatial distribution of emissions is seen, both versions just differ in the strength of the surface fluxes. Largest fluxes are concentrated in the Midwest, coinciding with the Corn Belt and its dominant agricultural emissions. Figure 2b shows DayCent direct soil emissions in July 2015. Similar to EDGAR, the Midwest is a prominent source of N_2O. We are not able to perform a detailed comparison of the spatial distributions in EDGAR and DayCent as both do not cover the same set of sources. However, in terms of the overall magnitude, DayCent estimates much higher surface fluxes compared to EDGAR, despite containing fewer sources (gridded total agricultural DayCent emissions are not available; Section 2.3).

Figure 2c displays the monthly evolution of E_{AGR}, E_{nonAGR}, and E_N averaged over the Midwest. Both EDGAR versions have an annual average E_{AGR} of ~0.10 nmol m^{-2} s^{-1}. However, unlike EDGAR5.0, EDGAR4.3.2 exhibits a strong seasonal cycle ranging from 0.05 nmol m^{-2} s^{-1} in winter up to 0.24 nmol m^{-2} s^{-1} in spring. In spring, when most N-fertilizer is applied, the amount peaks, followed by a plateau during summer at 0.09 nmol m^{-2} s^{-1}. The harvest season in fall features a local peak at 0.11 nmol m^{-2} s^{-1}. A future update of EDGAR5.0 will contain a seasonal cycle for some crop related emissions (Crippa et al., 2020). E_{nonAGR} shows no significant change over the year and is on average 0.04 nmol m^{-2} s^{-1} in both versions. Natural soil emissions account for 0.02 nmol m^{-2} s^{-1} per month.

From 2011 to 2015 DayCent emissions in the Midwest range between 0.23 and 0.35, 0.12–0.21, and 0.06–0.08 nmol m^{-2} s^{-1} in June, July, and October, respectively. June and July emissions are significantly larger than in EDGAR, despite excluding manure management, indirect soil, and agricultural waste burning emissions. DayCent's October emissions are within the magnitude of agricultural EDGAR emissions. We estimate total agricultural Midwest emissions from 2011 to 2015 by combining DayCent direct soil emissions and the EPA GHG inventory (Section 2.3), resulting in 0.32–0.48, 0.16–0.30, and 0.08–0.11 nmol m^{-2} s^{-1} in June, July, and October, respectively. In June/July this is on average over four/two times higher than EDGAR's E_{AGR}. The 2012 emissions are significantly lower than in the other years causing the large range across years in the summer months. During this year, the most extensive drought since the 1930s occurred across a large swath of the U.S., including most of the Midwest, which lead to widespread harvest failure (NOAA-NCEI, 2020). This event might explain the low values and indicates that during an average climatological year DayCent emissions are at the upper end of the range. Furthermore, in contrast to EDGAR4.3.2 which states constant emissions in June and July, DayCent emissions are much higher in June than in July. Sweeney et al. (2015) derived annual N_2O climatologies at Midwest sites from NOAA/ESRL Aircraft Network measurements and found highest N_2O mole fractions in June, consistent with our DayCent estimates.

3.2. Model Optimization

Here, we provide an example of the model optimization process for October 10, 2017 (Figure 3a). In the eastern part of the Midwest, N_2O enhancements up to 7 ppb were observed within the PBL. The below background values at the beginning of the time series occurred prior to the PBL transect in the free troposphere. Free tropospheric air might have a different history and hence different background which can lead to negative values if we subtract the PBL background. Model simulations with unmodified EDGAR emissions show only enhancements up to 1 ppb along the transect. However, by applying a correction factor F_{AGR} of 8.3 the model is able to reproduce our measurements. Optimizations of the remaining days can be found in the SI.

Figure 3b shows the mean and standard deviation for F_{AGR} of the Monte Carlo simulations of the 10 research flights for the two EDGAR versions. As both inventories have a comparable spatial distribution, factors vary due to differences in total emissions. EDGAR4.3.2 correction factors are considerably higher for October 2017 and slightly higher for June/July 2019 than EDGAR5.0. For EDGAR4.3.2, F_{AGR} ranges from 2.9 ± 1.5 to 11.3 ± 3.8 in 2017, with an average factor of 6.3 ± 4.6. EDGAR5.0 F_{AGR} is calculated to be lower, ranging from 1.6 ± 0.8 to 6.8 ± 2.3, with an average factor of 3.5 ± 2.7. For 2019 we modified EDGAR4.3.2 with a F_{AGR} between 5.5 ± 2.1 and 20.2 ± 6.3 and EDGAR5.0 between 4.9 ± 1.9 and 17.4 ± 5.5. On average this denotes an agricultural correction factor of 11.4 ± 6.6 and 9.9 ± 5.7 for EDGAR4.3.2 and EDGAR5.0, respectively. Altogether, both EDGAR versions exhibit a significant underestimation of agricultural emissions. Seasonal differences are likely one cause for the difference in correction factors between 2017 and 2019. Additionally, during the 2019 aircraft campaign, an extreme flooding event occurred that likely influenced our results (discussed below). Although EDGAR4.3.2 exhibits a seasonal cycle, its agricultural correction factor also varies considerably between 2017 and 2019. Hence, the Midwest seasonality is not captured in the EDGAR inventory, which appears to be caused by the flooding. Figure 3c displays the EDGAR5.0 average Midwest emissions for each flight with nonoptimized and optimized agricultural emissions. For EDGAR4.3.2, the optimized result is (nearly) the same as both versions differ (nearly) only in their strength of E_{AGR} which is adjusted in the course of the optimization. On average, optimized total N_2O emissions are 0.42 ± 0.28 nmol m^{-2} s^{-1} during our October 2017 and 1.06 ± 0.57 nmol m^{-2} s^{-1} during our June/July 2019 flights.

Optimized emissions for June/July 2019 are 2–3 times higher compared to DayCent emissions. Despite this, DayCent emissions are closer to our optimized emissions compared to EDGAR during the same period. In contrast, DayCent and EDGAR emissions are both too low by a similar magnitude in October compared to our optimized results. Hence, as DayCent considers regional characteristics, it performs much better on the regional scale in the summer than the emission factor approach that is used in EDGAR. A more quantitative evaluation of DayCent would require flux calculations for 2017 and 2019 incorporating the corresponding regional conditions like weather, soil conditions, and N-fertilizer application rate and time. DayCent has not been applied to estimate emissions specific to 2017 and 2019 so it is not clear if the model would underestimate the values for these years although this may be the case given the historical data from 2011 to 2015.

Fu et al. (2017) reported emissions of 3.00–4.38 nmol m^{-2} s^{-1} during June 1–20, 2010 for the Corn Belt, which is significantly higher than our estimates for June/July 2019. Griffis et al. (2013) estimated the Corn Belt emissions to be around 2 and 1 nmol m^{-2} s^{-1} in June/July 2010 and 2011, respectively, which is consistent with our findings. Kort et al. (2008) and Miller et al. (2012) derived scaling factors for the central U.S. To be able to compare their results to ours, we estimated the corresponding flux densities for the Midwest region using their scaling factors for the respective EDGAR versions. Kort et al. (2008) derived 0.54 nmol m^{-2} s^{-1} for May/June 2003 and Miller et al. (2012) 0.57/0.25 and 0.94/0.53 nmol m^{-2} s^{-1} for June/July 2004 and 2008, respectively. Both studies show lower values than our estimate. Miller et al. (2012) stated that maximum emissions occurred in June. Our DayCent calculations are also highest in June. This could partly explain our lower estimates compared to Fu et al. (2017) as we report for the end of June/beginning of July after the expected emission peak. Moreover, Fu et al. (2017) only scaled Corn Belt emissions and kept other regions unmodified which could lead to higher estimates, if they sampled other regions with lower emission rates than the Corn Belt. Overall, our estimates are in the range of previous top-down studies. However, the spread among the studies is large.

The nature of soil N_2O fluxes leads to significant temporal variability in the emissions that is not represented in EDGAR. DayCent is capable of representing those variations to a certain extent. For instance, precipitation events may enhance N_2O soil emissions (Butterbach-Bahl et al., 2013). DayCent has the potential to simulate such events since it considers meteorology. In October 2017 and June/July 2019, Midwest precipitation amounts were above-average, which probably enhanced N_2O emissions (see SI and NOAA, 2020a). Especially in 2019, weather conditions in the study domain were unusually extreme. During the campaign, the U.S. was experiencing its wettest period in 125 years, with severe flooding in the Midwest (NOAA, 2020b) forcing the farmers to significantly delay planting in the affected regions (USDA, 2020) and postponing the peak emission period. Depending on whether the zenith is shifted closer to or further away from our investigated period this event may have either amplified or lowered our emission estimates. Additionally, the above-average humidity might have enhanced soil N_2O emissions leading to higher estimates (Butterbach-Bahl et al., 2013). As indirect N_2O emissions play an important role in the Midwest (Griffis et al., 2013, 2017; Turner et al., 2015), flooding-induced emissions pulses of indirect emissions from streams and rivers probably also boosted soil N_2O fluxes (see SI). The influence of this flooding event cannot be quantified within this study, as this would require more data over longer periods spanning the whole event. However, in a follow-up study we plan to use DayCent simulations driven with those flooding conditions to gain insights on how soil N_2O emissions were affected.

4. Conclusion

Unique continuous in-situ airborne N_2O measurements of 10 research flights were used to quantify N_2O emissions in the U.S. Midwest using a top-down approach. In October 2017, average emissions were 0.42 nmol m^{-2} s^{-1}. The agricultural portion was on average 6.3 times higher than in EDGAR4.3.2 and 3.5 times higher than in EDGAR5.0. June/July 2019 emissions were on average 1.06 nmol m^{-2} s^{-1}. For that, agricultural EDGAR4.3.2 fluxes have to be scaled by an average factor of 11.4. EDGAR5.0 performs better again, but still requires an agricultural scaling factor of 9.9. Uncertainties were on the order of 50 %. Our 2019 estimates were most likely influenced by an extreme flooding event, which is difficult to capture in EDGAR as the inventory uses a climatological average emissions data set. Agricultural soil emissions estimated with DayCent in 2011–2015 were 0.32–0.48, 0.16–0.30, and 0.08–0.11 nmol m^{-2} s^{-1} in June, July, and October, respectively. These historical emission estimates are higher than nonoptimized EDGAR emissions,

but still significantly lower than our optimized fluxes. Our findings are in the range of previous top-down estimates for the Corn Belt and central U.S. However, a quantitative comparison of those studies shows that the range of derived N_2O surface fluxes is large, likely due to the temporal complexity of N_2O soil emissions.

More studies focusing on N_2O are necessary to fully understand the drivers of Midwest N_2O emissions and the most appropriate modeling methods to estimate emission patterns. To cover the high temporal variability on various scales, long-term projects with regular airborne measurements spanning wide areas of the Midwest are necessary. Combining a process-based model like DayCent capable of simulating the temporal and spatial variability of N_2O emissions, with extensive airborne and tall tower top-down studies at selected spots and times, could be a cost-effective approach that would limit the number of flights needed to produce accurate estimates for the region and improve national reporting of emissions (Ogle et al., 2020). As interest grows in expanding efforts to reduce N_2O emissions (Kanter et al., 2020), improved quantification of N_2O surface fluxes is mandatory for policy makers to be able to develop effective mitigation strategies.

Data Availability Statement

All ACT-America flask and in situ data used in this manuscript can be found online (at https://daac.ornl.gov/cgi-bin/dataset_lister.pl?p=37 and https://act-america.larc.nasa.gov/).

Acknowledgments
The ACT-America project is a NASA Earth Venture Suborbital-2 project funded by NASA's Earth Science Division (grant NNX15AG76G to the Pennsylvania State University). The authors thank DLR VO-R for funding the young investigator research group "Greenhouse Gases". This work used resources of the Deutsches Klimarechenzentrum (DKRZ) granted by its Scientific Steering Committee (WLA) under project ID bd1104. We also acknowledge funding from BMBF (German Federal Ministry of Education and Research) under project "AIRSPACE" (grant-no. FKZ01LK170). Open access funding enabled and organized by Projekt DEAL.

References

Baier, B. C., Sweeney, C., Choi, Y., Davis, K. J., DiGangi, J. P., Feng, S., et al. (2020). Multispecies assessment of factors influencing regional CO_2 and CH_4 enhancements during the winter 2017 ACT-America Campaign. *Journal of Geophysical Research: Atmospheres*, *125*, e2019JD031339. https://doi.org/10.1029/2019JD031339

Barkley, Z. R., Davis, K. J., Feng, S., Balashov, N., Fried, A., DiGangi, J., et al. (2019). Forward modeling and optimization of methane emissions in the South Central United States using aircraft transects across frontal boundaries. *Geophysical Research Letters*, *46*, 13564–13573. https://doi.org/10.1029/2019gl084495

Barkley, Z. R., Lauvaux, T., Davis, K. J., Deng, A., Fried, A., Weibring, P., et al. (2019). Estimating methane emissions from underground coal and natural gas production in Southwestern Pennsylvania. *Geophysical Research Letters*, *46*, 4531–4540. https://doi.org/10.1029/2019GL082131

Barkley, Z. R., Lauvaux, T., Davis, K. J., Deng, A., Miles, N. L., Richardson, S. J., et al. (2017). Quantifying methane emissions from natural gas production in north-eastern Pennsylvania. *Atmospheric Chemistry and Physics*, *17*(22), 13941–13966. https://doi.org/10.5194/acp-17-13941-2017

Butterbach-Bahl, K., Baggs, E. M., Dannenmann, M., Kiese, R., & Zechmeister-Boltenstern, S. (2013). Nitrous oxide emissions from soils: How well do we understand the processes and their controls? *Philosophical Transactions of the Royal Society B: Biological Sciences*, *368*, 20130122. https://doi.org/10.1098/rstb.2013.0122

Chen, Z., Griffis, T. J., Millet, D. B., Wood, J. D., Lee, X., Baker, J. M., et al. (2016). Partitioning N_2O emissions within the U.S. Corn Belt using an inverse modeling approach. *Global Biogeochemical Cycles*, *30*, 1192–1205. https://doi.org/10.1002/2015gb005313

Ciais, P., Sabine, C., Bala, G., Bopp, L., Brovkin, V., Canadell, J., et al. (2013). Carbon and other biogeochemical cycles. In T. F. Stocker, D. Qin, G.-K. Plattner, M. Tignor, S. K. Allen, J. Boschung, et al. (Eds.), *Climate change 2013: The physical science basis. Contribution of working group I to the fifth assessment report of the intergovernmental panel on climate change* (pp. 465–570). Cambridge: Cambridge University Press.

Crippa, M., Solazzo, E., Huang, G., Guizzardi, D., Koffi, E., Muntean, M., et al. (2020). High resolution temporal profiles in the emissions database for global atmospheric research. *Scientific Data*, *7*, 121. https://doi.org/10.1038/s41597-020-0462-2

Del Grosso, S. J., Parton, W. J., Keough, C. A., & Reyes-Fox, M. (2011). Special features of the DayCent modeling package and additional procedures for parameterization, calibration, validation, and applications. In L. R. Ahuja, & L. Ma (Eds.), *Methods of introducing system models into agricultural research* (pp. 155–176). Madison, WI: American Society of Agronomy, Crop Science Society of America, Soil Science Society of America. https://doi.org/10.2134/advagricsystmodel2.c5

Del Grosso, S. J., Parton, W. J., Mosier, A. R., Hartman, M. D., Brenner, J., Ojima, D. S., & Schimel, D. S. (2001). Simulated interaction of carbon dynamics and nitrogen trace gas fluxes using the DAYCENT model. In M. Schaffer, L. Ma, & S. Hansen (Eds.), *Modeling carbon and nitrogen dynamics for soil management* (pp. 303–332). Boca Raton, FL: CRC Press.

Díaz-Isaac, L. I., Lauvaux, T., & Davis, K. J. (2018). Impact of physical parameterizations and initial conditions on simulated atmospheric transport and CO_2 mole fractions in the US Midwest. *Atmospheric Chemistry and Physics*, *18*(20), 14813–14835. https://doi.org/10.5194/acp-18-14813-2018

EDGAR. (2020). *Emission database for global atmospheric research*. Retrieved from https://edgar.jrc.ec.europa.eu/

EDGAR4.3.2. (2017). *Emissions database for global atmospheric research, version 4.3.2*. European Commission. Retrieved from https://edgar.jrc.ec.europa.eu/overview.php?v%3D432_GHG; https://data.europa.eu/doi/10.2904/JRC-DATASET-EDGAR

EDGAR5.0. (2019). *Emissions database for global atmospheric research, version 5.0*. European Commission. Retrieved from https://edgar.jrc.ec.europa.eu/overview.php?v%3D50_GHG; https://data.europa.eu/doi/10.2904/JRC-DATASET-EDGAR

EPA. (2020). *Inventory of U.S. greenhouse gas emissions and sinks: 1990–2018 (EPA 430-R-20-002)*. United States Environmental Protection Agency. Retrieved from https://www.epa.gov/ghgemissions/inventory-us-greenhouse-gas-emissions-and-sinks-1990-2018

ERA5. (2017). *Copernicus climate change service (C3S)ERA5: Fifth generation of ECMWF atmospheric reanalyses of the global climate. Copernicus climate change service climate data Store (CDS)*. Retrieved from https://cds.climate.copernicus.eu/cdsapp#!/home

FAO. (2020). *Food and Agriculture Organization of the United Nations—FAOSTAT*. Retrieved from http://www.fao.org/faostat/en/#compare

Fu, C., Lee, X., Griffis, T. J., Dlugokencky, E. J., & Andrews, A. E. (2017). Investigation of the N_2O emission strength in the U.S. Corn Belt. *Atmospheric Research*, *194*, 66–77. https://doi.org/10.1016/j.atmosres.2017.04.027

GDAS-FNL. (2015). *National Centers for Environmental Prediction, National Weather Service, NOAA, U.S. Department of Commerce: NCEP GDAS/FNL 0.25 Degree Global Tropospheric Analyses and Forecast Grids*, updated daily. Research Data Archive at the National Center for Atmospheric Research, Computational and Information Systems Laboratory. https://doi.org/10.5065/D65Q4T4Z

Grell, G. A., Peckham, S. E., Schmitz, R., McKeen, S. A., Frost, G., Skamarock, W. C., & Eder, B. (2005). Fully coupled "online" chemistry within the WRF model. *Atmospheric Environment*, *39*(37), 6957–6975. https://doi.org/10.1016/j.atmosenv.2005.04.027

Griffis, T. J., Chen, Z., Baker, J. M., Wood, J. D., Millet, D. B., Lee, X., et al. (2017). Nitrous oxide emissions are enhanced in a warmer and wetter world. *Proceedings of the National Academy of Sciences of the United States of America*, *114*(45), 12081–12085. https://doi.org/10.1073/pnas.1704552114

Griffis, T. J., Lee, X., Baker, J. M., Russelle, M. P., Zhang, X., Venterea, R., & Millet, D. B. (2013). Reconciling the differences between top-down and bottom-up estimates of nitrous oxide emissions for the U.S. Corn Belt. *Global Biogeochemical Cycles*, *27*, 746–754. https://doi.org/10.1002/gbc.20066

Hall, B. D., Dutton, G. S., & Elkins, J. W. (2007). The NOAA nitrous oxide standard scale for atmospheric observations. *Journal of Geophysical Research*, *112*, D09305. https://doi.org/10.1029/2006JD007954

Hersbach, H., Bell, B., Berrisford, P., Hirahara, S., Horányi, A., Muñoz Sabater, J., et al. (2020). The ERA5 global reanalysis. *Quarterly Journal of the Royal Meteorological Society*, *146*, 1999–2049. https://doi.org/10.1002/qj.3803

Janssens-Maenhout, G., Crippa, M., Guizzardi, D., Muntean, M., Schaaf, E., Dentener, F., et al. (2019). EDGAR v4.3.2 Global Atlas of the three major greenhouse gas emissions for the period 1970–2012. *Earth System Science Data*, *11*(3), 959–1002. https://doi.org/10.5194/essd-11-959-2019

Kanter, D. R., Ogle, S. M., & Winiwarter, W. (2020). Building on Paris: Integrating nitrous oxide mitigation into future climate policy. *Current Opinion in Environmental Sustainability*, *47*, 7–12. https://doi.org/10.1016/j.cosust.2020.04.005

Kort, E. A., Eluszkiewicz, J., Stephens, B. B., Miller, J. B., Gerbig, C., Nehrkorn, T., et al. (2008). Emissions of CH_4 and N_2O over the United States and Canada based on a receptor-oriented modeling framework and COBRA-NA atmospheric observations. *Geophysical Research Letters*, *35*, L18808. https://doi.org/10.1029/2008GL034031

Kostinek, J., Roiger, A., Davis, K. J., Sweeney, C., DiGangi, J. P., Choi, Y., et al. (2019). Adaptation and performance assessment of a quantum and interband cascade laser spectrometer for simultaneous airborne in situ observation of CH_4, C_2H_6, CO_2, CO and N_2O. *Atmospheric Measurement Techniques*, *12*(3), 1767–1783. https://doi.org/10.5194/amt-12-1767-2019

MacFarling Meure, C., Etheridge, D., Trudinger, C., Steele, P., Langenfelds, R., van Ommen, T., et al. (2006). Law Dome CO_2, CH_4 and N_2O ice core records extended to 2000 years BP. *Geophysical Research Letters*, *33*, L14810. https://doi.org/10.1029/2006GL026152

Miller, S. M., Kort, E. A., Hirsch, A. I., Dlugokencky, E. J., Andrews, A. E., Xu, X., et al. (2012). Regional sources of nitrous oxide over the United States: Seasonal variation and spatial distribution. *Journal of Geophysical Research*, *117*, D06310. https://doi.org/10.1029/2011JD016951

Myhre, G., Shindell, D., Bréon, F.-M., Collins, W., Fuglestvedt, J., Huang, J., et al. (2013). Anthropogenic and natural radiative forcing. In T. F.Stockeret al. (Eds.), *Climate change 2013: The physical science basis. Contribution of working group I to the fifth assessment report of the intergovernmental panel on climate change* (pp. 659–740). Cambridge: Cambridge University Press.

NARR. (2005). *National Centers for Environmental Prediction*. National Weather Service, NOAA, U.S. Department of Commerce NCEP North American Regional Reanalysis, updated monthly. Research Data Archive at the National Center for Atmospheric Research, Computational and Information Systems Laboratory. Retrieved from https://rda.ucar.edu/datasets/ds608.0

NOAA. (2020). *National Centers for Environmental Information, climate at a glance: Regional mapping*. Retrieved from https://www.ncdc.noaa.gov/cag/

NOAA. (2020). *National Centers for Environmental Information, climate at a glance: Regional rankings*. Retrieved from https://www.ncdc.noaa.gov/cag/

NOAA-ESRL. (2020). *Combined nitrous oxide data from the NOAA/ESRL global monitoring division*. Retrieved from https://www.esrl.noaa.gov/gmd/hats/combined/N2O.html

NOAA-NCEI. (2020). *U.S. Billion-dollar weather and climate disasters*. NOAA National Centers for Environmental Information (NCEI). Retrieved from https://www.ncdc.noaa.gov/billions/

Ogle, S. M., Butterbach-Bahl, K., Cardenas, L., Skiba, U., & Scheer, C. (2020). From research to policy: Optimizing the design of a national monitoring system to mitigate soil nitrous oxide emissions. *Current Opinion in Environmental Sustainability*, *47*, 28–36. https://doi.org/10.1016/j.cosust.2020.06.003

Olivier, J. G. J., Bouwman, A. F., Berdowski, J. J. M., Veldt, C., Bloos, J. P. J., Visschedijk, A. J. H., et al. (1999). Sectoral emission inventories of greenhouse gases for 1990 on a per country basis as well as on 1°×1°. *Environmental Science and Policy*, *2*(3), 241–263. https://doi.org/10.1016/s1462-9011(99)00027-1

Olivier, J. G. J., Bouwman, A. F., van der Maas, C. W. M., Berdowski, J. J. M., Veldt, C., Bloos, J. P. J., et al. (1996). *Description of EDGAR version 2.0: A set of global emission inventories of greenhouse gases and ozone-depleting substances for all anthropogenic and most natural sources on a per country basis and on 1°×1°grid*. National Institute of Public Health and the Environment (RIVM) report no. 771060 002/TNO-MEP report no. R96/119. Retrieved from http://hdl.handle.net/10029/10497

Park, S., Croteau, P., Boering, K. A., Etheridge, D. M., Ferretti, D., Fraser, P. J., et al. (2012). Trends and seasonal cycles in the isotopic composition of nitrous oxide since 1940. *Nature Geoscience*, *5*(4), 261–265. https://doi.org/10.1038/ngeo1421

Parton, W. J., Hartman, M., Ojima, D., & Schimel, D. (1998). DAYCENT and its land surface submodel: Description and testing. *Global and Planetary Change*, *19*(1), 35–48. https://doi.org/10.1016/S0921-8181(98)00040-X

Paustian, K., Lehmann, J., Ogle, S. M., Reay, D., Robertson, G. P., & Smith, P. (2016). Climate-smart soils. *Nature*, *532*, 49–57. https://doi.org/10.1038/nature17174

Prather, M. J., Hsu, J., DeLuca, N. M., Jackman, C. H., Oman, L. D., Douglass, A. R., et al. (2015). Measuring and modeling the lifetime of nitrous oxide including its variability. *Journal of Geophysical Research: Atmospheres*, *120*, 5693–5705. https://doi.org/10.1002/2015jd023267

Ravishankara, A. R., Daniel, J. S., & Portmann, R. W. (2009). Nitrous oxide (N_2O): The dominant ozone-depleting substance emitted in the 21st century. *Science*, *326*(5949), 123–125. https://doi.org/10.1126/science.1176985

Reay, D. S., Davidson, E. A., Smith, K. A., Smith, P., Melillo, J. M., Dentener, F., & Crutzen, P. J. (2012). Global agriculture and nitrous oxide emissions. *Nature Climate Change*, *2*(6), 410–416. https://doi.org/10.1038/nclimate1458

Stehfest, E., & Bouwman, L. (2006). N_2O and NO emission from agricultural fields and soils under natural vegetation: Summarizing available measurement data and modeling of global annual emissions. *Nutrient Cycling in Agroecosystems*, *74*(3), 207–228. https://doi.org/10.1007/s10705-006-9000-7

Sweeney, C., Baier, B. C., Miller, J. B., Lang, P., Miller, B. R., Lehman, S., et al. (2018). ACT-America: L2 in situ atmospheric gas concentrations from Flasks, Eastern USA. *ORNL Distributed Active Archive Center*. Retrieved from https://daac.ornl.gov/cgi-bin/dsviewer.pl?ds_id%3D1575; https://doi.org/10.3334/ORNLDAAC/1575

Sweeney, C., Karion, A., Wolter, S., Newberger, T., Guenther, D., Higgs, J. A., et al. (2015). Seasonal climatology of CO_2 across North America from aircraft measurements in the NOAA/ESRL Global Greenhouse Gas Reference Network. *Journal of Geophysical Research: Atmospheres*, *120*, 5155–5190. https://doi.org/10.1002/2014jd022591

Thompson, R. L., Lassaletta, L., Patra, P. K., Wilson, C., Wells, K. C., Gressent, A., et al. (2019). Acceleration of global N_2O emissions seen from two decades of atmospheric inversion. *Nature Climate Change*, *9*(12), 993–998. https://doi.org/10.1038/s41558-019-0613-7

Tian, H., Xu, R., Canadell, J. G., Thompson, R. L., Winiwarter, W., Suntharalingam, P., et al. (2020). A comprehensive quantification of global nitrous oxide sources and sinks. *Nature*, *586*, 248–256. https://doi.org/10.1038/s41586-020-2780-0

Turner, P. A., Griffis, T. J., Lee, X., Baker, J. M., Venterea, R. T., & Wood, J. (2015). Indirect nitrous oxide emissions from streams within the US Corn Belt scale with stream order. *Proceedings of the National Academy of Sciences of the United States of America*, *112*(32), 9839–9843. https://doi.org/10.1073/pnas.1503598112

USDA. (2020). *Economics, statistics and market information system—Crop Progress*. Retrieved from https://usda.library.cornell.edu/concern/publications/8336h188j?locale=en#release-items

USDA-NASS. (2020). *United States Department of Agriculture—National Agricultural Statistics Service—Statistics by State*. Retrieved from https://www.nass.usda.gov/Statistics_by_State/index.php